Redox Driven Crystalline Coherent-Incoherent Transformation for a 2 ML VO_x Film Grown on α-TiO_2(110)

Chang-Yong Kim,*,† Jeffrey W. Elam,‡ Peter C. Stair,§ and Michael J. Bedzyk∥,⊥

Canadian Light Source, 101 Perimeter Road, Saskatoon, SK S7N 0X4, Canada, Energy Systems Division, Argonne National Laboratory, 9700 South Cass Avenue, Argonne, Illinois 60439, United States, Department of Chemistry, Northwestern University, 2145 Sheridan Road, Evanston, Evanston, Illinois 60208, United States, Department of Materials Science and Engineering, Northwestern University, 2220 Campus Drive, Evanston, Illinois 60208, United States, and Department of Physics and Astronomy, Northwestern University, 2145 Sheridan Road, Evanston, Illinois 60208, United States

Received: May 31, 2010; Revised Manuscript Received: October 5, 2010

A redox induced structural transformation for 2 monolayers of vanadia on α-TiO_2(110) (rutile) was studied by in situ X-ray standing waves and ex situ X-ray photoelectron spectroscopy. The VO_X film was grown by atomic layer deposition. Oxidation and reduction were carried out by annealing in O_2 and H_2, respectively. We found that an epitaxial rutile VO_2 film was formed in the reduced phase with V^{4+} cations in lateral alignment with Ti lattice positions. Oxidation was found to produce V^{5+} cations uncorrelated to the substrate lattice in the oxidized phase. The redox induced structural and oxidation state transformation proved reversible and involved the entire film; not just the surface layer. The current study suggests that the structural order needs to be considered in order to study the activity of supported vanadium oxide catalysts.

Introduction

Vanadium oxides have a wide range of applications in heterogeneous catalysis.[1−4] Thin epitaxial vanadium oxide films, from submonolayer to several layers thick, grown on various single-crystal oxide substrates can serve as model systems to study catalytic reactions on vanadium oxides.[5−16] Interestingly, submonolayer vanadium oxide films have shown a greater degree of chemical activity than multilayer or poorly ordered films.[5,7,8] Accessibility to V−O−S (where S represents the substrate cation) and the presence of surface V^{5+} have been considered crucial for the high activity of submonolayer films; in contrast to V^{4+} being observed in films at higher coverage (>1 monolayer).[7,8] Wang et al.[7] have attributed reduced activity in multilayer films to the existence of V^{4+}. While, Li and Altman[8] reported that multilayer epitaxial films retained dehydrogenation activity regardless of the existence of V^{4+} in the bulk of a multilayer film and suggested poor ordering or the formation of V_2O_5 clusters in the multilayer films of the previous studies as being the main reason for the discrepancy. In contrast to the epitaxial films on single-crystal substrates, multilayers of amorphous vanadium oxide (V^{5+} oxidation state) supported over TiO_2 powder have been observed by high resolution electron microscopy.[17,18] Considering the high activities observed from the multilayer amorphous vanadium oxides supported on oxide powders,[4,19] the existence of surface V^{5+} in the noncrystalline phase could be the key to activity in multilayer epitaxial films. During actual catalytic reactions, different oxidation states of vanadium coexist on the surface and this complicates analysis. Characterization of the electronic and atomic-scale structure of vanadium oxide in its pure state, either entirely reduced or oxidized, may provide insight into the behavior of vanadium oxide during practical catalytic reactions. Specifically, a study of the atomic-scale structural changes within a multilayer epitaxial vanadium oxide film at various stages during the oxidation−reduction process may help explain the reduced activity beyond 1 monolayer (ML).

Epitaxial vanadium oxide films have been grown by various methods, for example molecular beam epitaxy (MBE),[8−11,14] pulsed laser deposition (PLD),[20] hydrolysis,[6,7] and magnetron sputter deposition.[12] For MBE grown vanadium oxide, deposition of the V under reactive oxidation conditions produced more crystalline films than grown by post oxygen annealing of predeposited vanadium metal films.[11,13,21] For vanadium oxide films grown on α-TiO_2(110) substrates, growth of V_2O_3, VO_2,[8,11] and V_2O_5[8,21] have been reported. During the oxidation−reduction process, vanadium oxide films have shown reversible oxidation state changes of $V^{5+} \leftrightarrow V^{3+}$ and $V^{5+} \leftrightarrow V^{4+}$. For growth of vanadium oxide films by MBE, special attention is required for controlling the stoichiometry and consequent oxidation state of the vanadium oxide film.[10,21] As a thin film growth method atomic layer deposition (ALD) utilizes self-terminating chemical reactions and has been used for the growth of exotic epitaxial oxide multilayers, conformal coating of small particles, and manufacturing of 3-dimensional structures within microelectronic devices.[22−24] Since the ALD grown vanadium oxide film has a fully oxidized V^{5+} form,[25−27] the ALD method can provide an alternative route for growing epitaxial VO_2 films through the postreduction of an as-grown vanadium oxide.

We previously reported that ALD grown submonolayer tungsten oxide on the rutile TiO_2(110) surface is highly coherent and isostructural to the TiO_2(110) substrate.[28] Also, the oxidation−reduction process of a submonolayer of vanadium oxide grown with MBE on α-Fe_2O_3(0001) was shown to cause a redistribution of the adsorbed vanadium.[14] Herein, we extend these previous studies by examining the oxidation−reduction

* To whom correspondence should be addressed.
† Canadian Light Source.
‡ Argonne National Laboratory.
§ Department of Chemistry, Northwestern University.
∥ Department of Materials Science and Engineering, Northwestern University.
⊥ Department of Physics and Astronomy, Northwestern University.

10.1021/jp104978a
Published on Web 10/28/2010

process of an ALD grown 2 ML VO_x film on TiO_2(110). The electronic and atomic structures of the ALD grown VO_x film in oxidized and reduced phases were studied with X-ray photoelectron spectroscopy (XPS) and X-ray standing wave (XSW) analysis.

Experimental Section

The 10 × 10 × 1 mm^3 single crystal rutile α-TiO_2(110) substrate (Crystal GmbH) was cleaned by annealing at 1050 °C under an oxygen flow followed by surface irradiation with UV light in 100% humidity environment. Prior to ALD growth, the sample was hydroxylated by immersion in boiling water, rinsed with HCl, and then blown dry with N_2. In the ALD process the sample was exposed to vanadyl oxytriisopropoxide (VOTP) flow at 100 °C for 10 min. The VOTP was purged with dry nitrogen gas and the sample was treated under H_2O_2 flow at 100 °C. After removal from the ALD reactor the as-grown VO_x sample was installed inside a beryllium dome oven that was mounted on a 4-circle diffractometer for XSW measurements at the Advanced Photon Source (APS) 12ID-D station. The Be-dome oven was equipped with a pyrolytic boron nitride (PBN) heater and gas inlet and outlet ports. The sample was held on the PBN heater surface by Pt−Ir alloy wires. Inside the Be-dome the VO_x sample was oxidized by annealing at 375 °C under a flowing O_2 environment and reduced by annealing at 275 °C under a flow of 2% H_2 in a helium carrier gas. For both gas-treatments the annealing time was 30 min and flow rate was c.a. 100 sccm. The sample temperature was measured by an R-type thermocouple attached to the sample securing Pt−Ir wire. During the XSW measurements the Be-dome sample chamber was pumped to a high vacuum.

The V coverage was determined to be 2.0 ML by comparing the V K X-ray fluorescence (XRF) yield from the sample to that of a calibrated standard. The XRF was measured with a silicon drift diode detector. We define 1 ML = 10.4 atoms/nm^2 which is the areal density of the Ti atoms in a (110) Ti atomic layer of bulk α-TiO_2. Each X-ray standing wave (XSW) measurement consisted of monitoring the V Kβ XRF modulation while scanning the diffractometer angle through an *hkl* substrate Bragg reflection.[29−32] The amplitude (f_H) and phase (P_H) of the $H = hkl$ Fourier component of the V atomic density distribution is directly extracted from this modulation of the V XRF yield. As recently demonstrated, a summation of an XSW measured set of *hkl* Fourier components generates a model-independent element-specific real-space 3D atomic map with respect to the substrate unit cell.[14,28,33−37] The Fourier amplitudes, f_H, which are also referred to as coherent fractions, measure the coherency of the XRF selected atom distribution with respect to the substrate lattice. A case where $f_H = 0$ for all *hkl* would correspond to a homogeneous (random) distribution as generated by the crystallographic projection of all XRF selected atoms into one substrate unit cell. At the other extreme, $f_H = 1$ corresponds to a distribution that when projected along that particular *H* direction has a single delta-function positioned at a fractional diffraction plane spacing of $\Delta d/d_H = P_H$.

X-ray photoelectron spectroscopy (XPS) measurements used an Al X-ray source (without monochromator), hemispherical electron energy analyzer and sample load-lock chamber. The base pressure of the XPS UHV chamber was 2 × 10^{-10} Torr. Oxidation and reduction of the VO_x film for the XPS measurements were conducted inside the load-lock chamber. The sample was heated by thermal radiation from a halogen lamp while the load-lock chamber was filled either with 1 atm O_2 gas or 20 Torr H_2 gas. The sample temperature was measured by a K-type thermocouple contacting the side of the sample. These gas pressures were maintained during sample cool-down periods. After the load-lock chamber was pumped down to 1 × 10^{-8} Torr, the sample was introduced back into the UHV chamber for the XPS measurements.

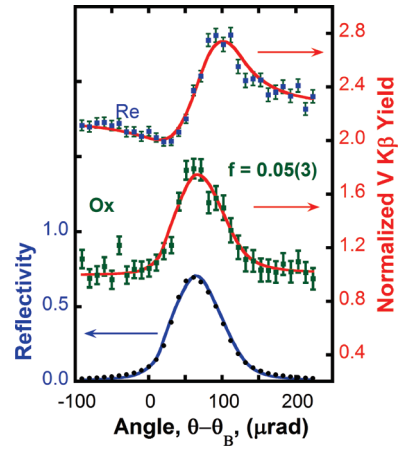

Figure 1. XSW data and analysis for the (110) reflection from TiO_2. Bottom: the TiO_2(110) substrate reflectivity. Middle: the V XRF modulation for the oxidized (Ox). Top: the reduced (Re) vanadium oxide films are shown. For clarity the V XRF modulation from the Re phase was shifted vertically. In the oxidized film the coherent fraction (*f*) was 0.05 ± 0.03.

Results and Discussion

The XSW analysis from the as-grown V-ALD film (not shown) did not show any coherence of the vanadium spatial distribution with respect to the underlying substrate lattice structure. This is understandable partially because the film deposition temperature was 100 °C during the ALD process, and ALD V_2O_5 films deposited under these conditions have been shown previously to be amorphous according to XRD.[27] The as-grown film was annealed under flowing O_2 at 340 °C to induce ordering in the vanadia layer. However, as shown in Figure 1 the (110) XSW analysis along the sample normal direction after the oxygen annealing (Ox) indicates a random vanadium distribution based on the very low measured value of f_{110}. The XSW measurement from the (101) off-specular reflection also showed a completely random V distribution (i.e., $f_{101} \sim 0$). No further XSW measurements from other nonspecular reflections were attempted.

As shown in Figure 1, ordering in the vanadium oxide film appeared after reduction (Re) of the oxidized surface by annealing under 2% H_2 flow at 270 °C. The O_2 and H_2 anneals were repeated several times and the V distribution was observed to change reversibly between incoherent (oxidized) and coherent (reduced).

The electronic structure of the oxidized and reduced vanadium oxide films were measured by XPS (Figure 2). In the binding energy range surrounding the O 1s and V 2p core levels, the measured spectra consist of photoelectrons (PE) from substrate oxygens, surface hydroxyl groups (OH^-), and from the vanadium oxide. To determine the oxidation state of the vanadium, line shape analysis was performed through nonlinear least-squares curve fitting to the measured spectra by the sum of individual PE lines that were represented by a Voigt functional form with a Shirley background contribution.[38,39] The PE lines were the vanadium $2p_{3/2}-2p_{1/2}$ doublet and O 1s contributed from the substrate oxygen and adsorbed OH^-. Because the Al X-ray source was used without a monochromator, the incident

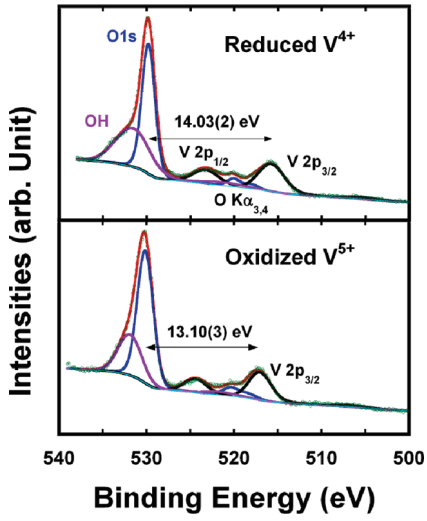

Figure 2. O 1s and V 2p XP spectra from the oxidized and reduced vanadium oxide films. The binding energy differences between O 1s and V $2p_{3/2}$ are indicated by arrows. The extra peaks near the binding energy of 520 eV correspond to the O 1s excited by the Al $K\alpha_{3,4}$.

TABLE 1: XSW Measured Phases (P_H) and Amplitudes (f_H) of hkl Fourier Components for the V Distribution of the Reduced Surface as Compared to Those Derived from a Calculation Based on a Best-Fit Model

hkl	*d* spacing(Å)	f_{meas}	f_{calc}	P_{meas}	P_{calc}
110	3.25	0.58(1)	0.45	0.93(1)	0.95
101	2.49	0.60(4)	0.61	0.99(2)	0.98
200	2.30	0.34(6)	0.45	1.03(4)	0.95
211	1.69	0.22(9)	0.23	0.88(6)	0.93

beam has Al $K\alpha_{3,4}$ X-rays in addition to the major $K\alpha_{1,2}$ radiation. Throughout the fit the ratio between photoelectron intensities excited by Al $K\alpha_{1,2}$ and $K\alpha_{3,4}$ are fixed to the intensity ratio of O 1s excited by $K\alpha_{1,2}$ and $K\alpha_{3,4}$ measured from a clean TiO_2(110) substrate. The binding energies of the V $2p_{3/2}$ are determined as 517.1 eV for the oxidized phase and 515.8 eV for the reduced phase. Reported values for various vanadium oxides are V^{3+} at 515.15−515.85 eV, V^{4+} at 515.65−516.2 and V^{5+} at 516.9−517.2 eV.[40−43] An unambiguous assignment for the oxidation state of the V is obtained by using the BE separation between and O 1s and V $2p_{3/2}$.[44] In the literature the BE differences are 14.84 eV for V^{3+}, 14.35 eV for V^{4+} and 12.8 eV for V^{5+}.[41] Our measured BE separations are 14.0 eV for the reduced and 13.1 eV for the oxidized phase. Hence the oxidation states of the vanadium can be assigned to 4+ for the reduced phase and 5+ for the oxidized phase. No noticeable change was observed in Ti 2p XP spectra after reduction and oxidation.

The XSW analysis listed in Table 1 shows a moderately high coherent structure for the vanadia in the reduced phase. The summation of these XSW measured Fourier components and their symmetry equivalents leads to a model-independent 3D V atomic density map shown in Figure 3. Due to the nature of the Fourier transform, the 3D atomic density map is forced to have the periodicity of the primitive unit cell.

The 3D V atomic distribution shows that V atoms in the surface overlayer occupy α-TiO_2 bulk-like Ti sites. The occupation of the bulk-like Ti sites was also observed in our earlier study of ALD grown 0.3 ML W on α-TiO_2(110).[28] Formation of a highly coherent VO_2 film isostructural to the TiO_2 rutile substrate has been reported in films grown by various methods.[9,10,12,13] To quantify the V adsorption geometry further,

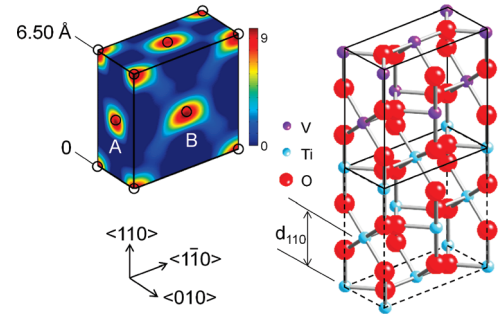

Figure 3. XSW measured 3D V atomic density map for the reduced surface. Open black circles denote the ideal bulk-like Ti lattice sites expected from the ideal extension of the support above the surface. The two symmetry inequivalent Ti sites are labeled as A and B. The V density maxima are laterally aligned with sites A and B, but shifted slightly downward. For comparison, a ball and stick model for the rutile VO_2 on rutile TiO_2 structure is shown at the right. In the ball and stick model the oxygens are presumed to occupy the same sites as in bulk rutile.

the XSW measured coherent fractions and positions were fit with a parametrized structural model. Since the measured V coverage was 2.0 ML, the structural model assumed two rutile-like pseudomorphic layers of V with the vertical offsets of two layers from the bulk-like positions used as the fitting parameters. The best fit gives an coherent occupation fraction of 0.66(9) for both V layers and heights of 2.7(1) Å and 6.8(1) Å (or 3.5(1) Å and 5.9(1) Å) for the bottom and top V layers with respect to the unperturbed topmost bulk TiO layer. Coherent occupation fraction of 0.66 means that in each layer 2/3 of vanadium occupies coherent or ordered position and 1/3 of V is incoherent to substrate either occupying defect sites of substrate or forming nanoparticle or disordered phase. Due to its inherent periodic ambiguity, the XSW results alone cannot distinguish between the two layer height pairs of (d_{110} + 0.29 Å, 2 × d_{110} − 0.59 Å) and (d_{110} + 0.59, 2 × d_{110} − 0.25) where d_{110} = 3.25 Å is the TiO_2 (110) *d* spacing. This ambiguity could be perhaps best resolved by X-ray crystal truncation rod measurements. Note that our XSW measured separation distance between VO layers (4.1(2) Å or 2.4(2) Å) significantly differs from the 3.22 Å found for bulk-like rutile VO_2.[45]

The XSW V map together with the XPS oxidation state and XRF coverage measurements indicate that in the reduced phase there are 2 monolayers of V^{4+} cations forming a VO_2 epitaxial rutile film that is pseudomorphic to the rutile TiO_2 structure. This is not surprising, since the room temperature bulk tetragonal-P lattice constants of a = 4.5546 Å and c = 2.8514 Å for the rutile phases of VO_2 are closely matched to that of TiO_2 (4.5937 Å and 2.9581 Å). For the oxidized phase the 2 ML of V^{5+} ions form an oxide structure that is uncorrelated (or out of registry) with the TiO_2 rutile lattice. For a submonolayer vanadium oxide film grown by ALD on α-TiO_2(110), XSW analysis of oxidized phase revealed a certain degree of order for V^{5+}.[46] The submonolayer vanadium can be considered as an adsorbate with well-defined adsorption sites on the rutile substrate. Beyond one monolayer coverage, an additional vanadium oxide begins to form over the first layer. If the V^{5+} forms tetrahedral VO_4 with bonds to three oxygen atoms below it would be difficult for the tetrahedra to assume a high symmetric sites and form an ordered phase on the 2-fold symmetric rectangular surface unit cell of TiO_2(110).[10,47] The V^{5+} film that XSW measurements find to be completely incoherent with the substrate can be an amorphous phase or can consist of crystalline grains or 3D nanoclusters that are

spatially uncorrelated with the substrate lattice. Losing structural coherence with the substrate beyond 1 ML of V^{5+} has been observed previously for vanadium oxide deposited on anatase (001).[48] Recently, Li et al. have reported that V^{4+} predominates in the bulk of MBE grown vanadium oxide multilayer films and a V^{5+} surface layer was formed after O_2 annealing in 1×10^{-8} Torr.[8] Annealing under ambient O_2 pressure could change V^{4+} in the bulk to V^{5+} up to a certain film thickness. Crystalline V_2O_5 is the typical form of V^{5+} appearing at high vanadium loadings on an oxide support, and it reduces the activity of vanadium oxide catalysts by blocking active sites.[1−4] The activity of the vanadium oxide supported on a powder has been observed to decrease after completion of about 4−5 layers of an amorphous film.[1−4] Our current study finds that the whole film, not just the surface layer, undergoes a reversible coherent - incoherent structural transformation associated with reduction - oxidation. The 4−5 ML could be a limiting film thickness for V^{5+} to maintain a disordered structure after an oxidation-induced transformation from the ordered V^{4+} phase. It is worthwhile to point out that oxidation condition of current study falls in the regime where V_2O_5 is the thermodynamically favored phase and there are no significant kinetic constraints under this condition to completely oxidizing the film, not just the surface. Under more general reaction conditions where the catalyst is exposed to both oxygen and a reducing hydrocarbon, a regime could be entered where bulk oxidation to V_2O_5 is not favored but rather phases such as V_3O_7[49] or V_4O_9[50] may predominate or where oxygen adsorption on more reduced phases can become feasible. Since the energetics and rates of chemical reactions will depend on the corresponding quantities in associated structural transformations changes in the oxide structure need to be considered for understanding the performance of supported catalysts.

In summary, an ALD grown 2 ML VO_X film on α-TiO_2(110) forms a well-ordered pseudomorphic epitaxial VO_2 film in the reduced phase and transforms to a disordered V^{5+} vanadium oxide after oxidation. The crystalline coherent-incoherent transformation is reversible as the oxidation state cycles between V^{4+} and V^{5+}.

Acknowledgment. This work was supported by the Chemical Sciences, Geosciences and Biosciences Division, Office of Basic Energy Sciences, Office of Science, U.S. Department of Energy under Contract W-31-109-ENG-38 and Grant DE-FG02-03ER15457. Use of the Advanced Photon Source was supported by the U.S. Department of Energy, Office of Science, Office of Basic Energy Sciences, under Contract No. DE AC02-06CH11357. This work made use of NU Central Facilities supported by the MRSEC through NSF Contract No. DMR-0520513.

References and Notes

(1) Wachs, I. E.; Weckhuysen, B. M. *Appl. Catal., A* **1997**, *157*, 67.
(2) Inumaru, K.; Misono, M.; Okuhara, T. *Appl. Catal., A* **1997**, *149*, 133.
(3) Weckhuysen, B. M.; Keller, D. E. *Catal. Today* **2003**, *78*, 25.
(4) Centi, G. *Appl. Catal., A* **1996**, *147*, 267.
(5) Wong, G. S.; Kragten, D. D.; Vohs, J. M. *Surf. Sci.* **2000**, *452*, L293.
(6) Wang, Q.; Madix, R. J. *Surf. Sci.* **2001**, *474*, L213.
(7) Wang, Q.; Madix, R. J. *Surf. Sci.* **2002**, *496*, 51.
(8) Li, M.; Altman, E. I. *J. Phys. Chem. C* **2009**, *113*, 2798.
(9) Della Negra, M.; Sambi, M.; Granozzi, G. *Surf. Sci.* **1999**, *436*, 227.
(10) Kroger, E. A.; Allegretti, F.; Knight, M. J.; Polcik, M.; Sayago, D. I.; Woodruff, D. P.; Dhanak, V. R. *Surf. Sci.* **2006**, *600*, 4813.
(11) Shinya, M.; Kentaro, A.; Masashi, N.; Masanori, O.; Yoshimasa, N. *Surf. Interface Anal.* **2008**, *40*, 1650.
(12) Sambi, M.; Sangiovanni, G.; Granozzi, G.; Parmigiani, F. *Phys. Rev. B* **1997**, *55*, 7850.
(13) Agnoli, S.; Sambi, M.; Granozzi, G.; Castellarin-Cudia, C.; Surnev, S.; Ramsey, M. G.; Netzer, F. P. *Surf. Sci.* **2004**, *562*, 150.
(14) Kim, C.-Y.; Escuadro, A. A.; Stair, P. C.; Bedzyk, M. J. *J. Phys. Chem. C* **2007**, *111*, 1874.
(15) Surnev, S.; Ramsey, M. G.; Netzer, F. P. *Prog. Surf. Sci.* **2003**, *73*, 117.
(16) Atrei, A.; Cecconi, T.; Cortigiani, B.; Bardi, U.; Torrini, M.; Rovida, G. *Surf. Sci.* **2002**, *513*, 149.
(17) Sanati, M.; Reine Wallenberg, L.; Andersson, A.; Jansen, S.; To, Y. *J. Catal.* **1991**, *132*, 128.
(18) Wallenberg, L. R.; Sanati, M.; Andersson, A. *J. Catal.* **1990**, *126*, 246.
(19) Poelman, H.; Silversmit, G.; Poelman, D.; Marin, G. B.; Sels, B. S. *Catal. Today* **2009**, *142*, 125.
(20) Ramana, C. V.; Smith, R. J.; Hussain, O. M.; Julien, C. M. *Mater. Sci. Eng., B* **2004**, *111*, 218.
(21) Wong, G. S.; Concepcion, M. R.; Vohs, J. M. *Surf. Sci.* **2003**, *526*, 211.
(22) Lakomaa, E. L. *Appl. Surf. Sci.* **1994**, *75*, 185.
(23) Suntola, T.; Simpson, M. *Atomic layer epitaxy*; Blackie: Glasgow, 1990.
(24) Elam, J. W.; Routkevitch, D.; Mardilovich, P. P.; George, S. M. *Chem. Mater.* **2003**, *15*, 3507.
(25) Keränen, J.; Auroux, A.; Ek, S.; Niinistö, L. *Appl. Catal., A* **2002**, *228*, 213.
(26) Keränen, J.; Auroux, A.; Ek-Härkönen, S.; Niinistö, L. *Thermochim. Acta* **2001**, *379*, 233.
(27) Musschoot, J.; Deduytsche, D.; Poelman, H.; Haemers, J.; Van Meirhaeghe, R. L.; Van den Berghe, S.; Detavernier, C. *J. Electrochem. Soc.* **2009**, *156*, P122.
(28) Kim, C.-Y.; Elam, J. W.; Pellin, M. J.; Goswami, D. K.; Christensen, S. T.; Hersam, M. C.; Stair, P. C.; Bedzyk, M. J. *J. Phys. Chem. B* **2006**, *110*, 12616.
(29) Golovchenko, J. A.; Patel, J. R.; Kaplan, D. R.; Cowan, P. L.; Bedzyk, M. J. *Phys. Rev. Lett.* **1982**, *49*, 560.
(30) Zegenhagen, J. *Surf. Sci. Rep.* **1993**, *18*, 199.
(31) Bedzyk, M. J.; Cheng, L. W. *Rev. Mineral. Geochem.* **2002**, *49*, 221.
(32) Woodruff, D. P. *Rep. Prog. Phys.* **2005**, *68*, 743.
(33) Cheng, L.; Fenter, P.; Bedzyk, M. J.; Sturchio, N. C. *Phys. Rev. Lett.* **2003**, *90*, 255503.
(34) Zhang, Z.; Fenter, P.; Cheng, L.; Sturchio, N. C.; Bedzyk, M. J.; Machesky, M. L.; Wesolowski, D. J. *Surf. Sci.* **2004**, *554*, L95.
(35) Okasinski, J. S.; Kim, C.-Y.; Walko, D. A.; Bedzyk, M. J. *Phys. Rev. B* **2004**, *69*, 041401.
(36) Kim, C.-Y.; Klug, J. A.; Stair, P. C.; Bedzyk, M. J. *J. Phys. Chem. C* **2009**, *113*, 1406.
(37) Feng, Z.; Kim, C.-Y.; Elam, J. W.; Ma, Q.; Zhang, Z.; Bedzyk, M. J. *J. Am. Chem. Soc.* **2009**, *131*, 18200.
(38) Shirley, D. A. *Phys. Rev. B* **1972**, *5*, 4709.
(39) Proctor, A.; Sherwood, P. M. A. *Anal. Chem.* **1982**, *54*, 13.
(40) Sawatzky, G. A.; Post, D. *Phys. Rev. B* **1979**, *20*, 1546.
(41) Mendialdua, J.; Casanova, R.; Barbaux, Y. *J. Electron Spectrosc. Relat. Phenom.* **1995**, *71*, 249.
(42) Demeter, M.; Neumann, M.; Reichelt, W. *Surf. Sci.* **2000**, *454−456*, 41.
(43) Silversmit, G.; Depla, D.; Poelman, H.; Marin, G. B.; De Gryse, R. *J. Electron Spectrosc. Relat. Phenom.* **2004**, *135*, 167.
(44) Coulston, G. W.; Thompson, E. A.; Herron, N. *J. Catal.* **1996**, *163*, 122.
(45) Mcwhan, D. B.; Marezio, M.; Remeika, J. P.; Dernier, P. D. *Phys. Rev. B* **1974**, *10*, 490.
(46) Feng, Z.; Kim, C.-Y.; Elam, J. W.; Bedzyk, M. J. to be published.
(47) Agnoli, S.; Castellarin-Cudia, C.; Sambi, M.; Surnev, S.; Ramsey, M. G.; Granozzi, G.; Netzer, F. P. *Surf. Sci.* **2003**, *546*, 117.
(48) Gao, W.; Wang, C. M.; Wang, H. Q.; Henrich, V. E.; Altman, E. I. *Surf. Sci.* **2004**, *559*, 201.
(49) Centi, G.; Granados, M. L.; Pinelli, D.; Trifiro, F.; Sleight, R. K. G. a. A. W. Redox Dynamics and Structure/Activity Relationships in Vanadium-Oxide on TiO2 Catalyst. In *Stud. Surf. Sci. Catal.*; Elsevier: Amesterdam, 1991; Vol. 67, p 1.
(50) Fiermans, L.; Clauws, P.; Lambrecht, W.; Vandenbroucke, L.; Vennik, J. *Phys. Status Solidi A* **1980**, *59*, 485.

JP104978A